Journal of Molecular Structure 1075 (2014) 32–42

Contents lists available at ScienceDirect

Journal of Molecular Structure

journal homepage: www.elsevier.com/locate/molstruc

Preparation, spectral studies, theoretical, electrochemical and antibacterial investigation of a new Schiff base and its some metal complexes

S. Ilhan [a,*], H. Baykara [a,*], M.S. Seyitoglu [a], A. Levent [b], S. Özdemir [c], A. Dündar [d], A. Öztomsuk [a], M.H. Cornejo [e]

[a] Faculty of Science and Letters, Chemistry Department, Siirt University, Siirt, Turkey
[b] Batman University, Health Services Vocational College, 72100 Batman, Turkey
[c] Faculty of Science and Letters, Biology Department, Siirt University, Siirt, Turkey
[d] Mardin Artuklu University, Vocational Higher School of Health Services, Medical Promotion and Marketing Program, 47000 Mardin, Turkey
[e] Escuela Superior Politécnica del Litoral, ESPOL, CIDNA, Km 30.5 Via Perimetral, Guayaquil, Ecuador

HIGHLIGHTS

- 1,6-Bis(2-(5-bromo-2-hydroxybenzylideneamino)-4-chlorophenoxy)hexane was synthesized.
- [CuL], [NiL], [CoL], [ZnL], [VLCl] complexes of the ligand were synthesized.
- In addition theoretical ^{1}H- NMR, HOMO–LUMO studies of the ligand were done.
- Antioxidant and antibacterial activities of the compounds were examined.

ARTICLE INFO

Article history:
Received 30 May 2014
Received in revised form 19 June 2014
Accepted 20 June 2014
Available online 26 June 2014

Keywords:
Di-functional ligand
Cyclic voltammetry
Antioxidant
HOMO–LUMO
Mass spectra and Gaussian

ABSTRACT

A new Schiff base ligand, 1,6-Bis(2-(5-bromo-2-hydroxybenzylideneamino)-4-chlorophenoxy)hexane was synthesized. Some Schiff metal complexes of the new Schiff base were prepared by the reaction of some metal salts and the Schiff base. The complexes are non-electrolytes as shown by their molar conductivities (ΛM). The structures of metal complexes are proposed from elemental analysis, FT-IR, UV–vis, magnetic susceptibility measurements, molar conductivity measurements, mass spectra and thermal gravimetric analysis. In addition theoretical ^{1}H NMR, HOMO–LUMO studies of the ligand; antimicrobial and cyclic voltammetric studies of the compounds were also carried out. In this study antioxidant and antibacterial activities of the compounds were examined via in vitro methods.

© 2014 Elsevier B.V. All rights reserved.

Introduction

Synthesis and characterization of Schiff bases and their corresponding complexes are very important because of their potential applications and properties such as anticancer, anticonvulsant, antitumor, antifungal, antibacterial, antitubercular, antioxidant, antimalarias, antiflammatory, corrosion inhibitor, biological, anti-HIV and pesticidal properties [1–19]. Through the years, Schiff bases played and developed a central role as chelating ligands in the main group and transition metal coordination chemistry [20–24].

Yorke et al. synthesized 2,4,6-trimethyl-(di-2-pyridylmethylene)aniline and 2,6-di-isopropyl-(di-2-pyridylmethylene)aniline via condensation reactions between 2,2′-dipyridyl ketone and 2,4,6-trimethylaniline and 2,6-di-isopropylaniline. They prepared palladium (II) complexes of the new imine compounds and used the complexes as catalysts in Suzuki coupling reaction of p-bromoanisole and phenylboronic acid [25].

Yang et al. described and explained the carbon–fluorine bond activation and alkylation in polyfluoroaryl Schiff bases by in situ ^{19}F NMR spectroscopy [26].

Pordel et al. synthesized and characterized novel 2-(5-hydroxyimino-1-alkyl-4,5-dihydro-1H-4-indazolyliden)-2-arylacetonitriles. They found out and showed the intramolecular charge transfer (ICT) due to their color intensities [27].

* Corresponding authors. Tel.: +90 4842231224; fax: +90 4842232086.
E-mail addresses: hacibaykara@gmail.com, salihsiirt@gmail.com (H. Baykara).

http://dx.doi.org/10.1016/j.molstruc.2014.06.062
0022-2860/© 2014 Elsevier B.V. All rights reserved.

Suvitha et al. synthesized pycolinaldehyde oxime (PAO) by the reaction of picolinaldehyde (2-formyl pyridine) with hydroxylamine. They carried out some comparative studies too by means of comparison of theoretical (B3LYP/6-311++G(d,p)) and experimental FT-IR and FT-Raman spectra, and theoretical NMR values to experimental values of PAO as supportive characterizations studies. On the other hand, frontier orbitals', HOMO–LUMO with their energies (by time-dependent DFT (TD-DFT)), molecular electrostatic potentials (MEP) were also visualized [28].

Kharadi synthesized octahedral copper complexes of clioquinol (CQ) and substituted terpyridine. Antimycobacterial properties of the complexes and the ligands were investigated against *Mycobacterium tuberculosis*. Antioxidant properties of the compounds were carried out by ferric-reducing method, and antimicrobial activities of the compounds were also investigated against five different microorganisms [29].

Dhanaraj and Johnson synthesized a Schiff base by the reaction of quinoxaline-2,3-(1,4H)-dione and 4-aminoantipyrine (QDAAP) then prepared its new metal complexes and investigated antimicrobial properties of the compounds synthesized [30].

Upadhyay et al. synthesized and characterized monomeric metal complexes, [Cu(L1)] and [Ni(L1)], by the reaction of Schiff (L1 = $C_{20}H_{24}NO_2$) base ligands with metal salts [31].

In this study, a new Schiff base, 1,6-Bis(2-(5-bromo-2-hydroxybenzylideneamino)-4-chlorophenoxy)hexane and its metal complexes were prepared and characterized. All of the compounds were characterized by several characterization techniques including FT-IR, ^{13}C NMR, ^{1}H NMR, UV–vis, magnetic susceptibility studies, theoretical studies, electrochemical, antioxidant and antimicrobial studies.

Experimental

Material and methods

All the chemicals and solvents were used as received, without a further purification. Elemental analyses were carried out on a LECO CHNS model 932 elemental analyze device. FT-IR spectra were recorded on a PERKIN ELMER SPECTRUM 100 FTIR spectrometer on a universal ATR arm. Ultraviolet–visible spectroscopic studies were done on a PERKIN ELMER LAMBDA 750 model UV Visible spectrophotometer in the wavelength. Molar conductivities were measured by using a Mettler Toledo Seven Multi pH Conductivity Meter.

^{1}H and ^{13}C NMR spectra were recorded using a BRUKER AVANCE DPX-400 NMR spectrometer. Magnetic Susceptibilities were measured by using a Sherwood Scientific Magnetic Susceptibility Balance (Model MK1) at room temperature (20 °C) using $Hg[Co(SCN)_4]$ as a calibrant; diamagnetic corrections were calculated from Pascal's constants [32]. Mass spectral analyses were determined on an Agilent 1100 Series LC/MSD mass spectrometer. Thermal stability properties were investigated on a EXSTAR S II TG/DTA 6300 Model thermal analyzer. A standard office computer (with 4 GB RAM) was used to carry out the theoretical calculations. Gaussian 09 and Gauss View 5 software packages were used for the optimization, theoretical ^{1}H NMR, frontier orbitals and visualization of the entire input and output files. Electrochemical experiments were carried out by using an Autolab PGSTAT 128 N potentiostat, with a three electrode system, glassy carbon working electrode (Φ: 3 mm, BAS), platinum wire as auxiliary electrode and Ag/AgCl (NaCl 3 M, Model RE-1, BAS, USA) as reference electrode. The reference electrode is separated from the bulk solution by a fritted-glass bridge filled with the solvent/supporting electrolyte mixture. Before starting each experiment, the glassy carbon electrode is polished manually with alumina (Φ: 0.01 μm). Cyclic voltammetric (CV) experiments are recorded at room temperature in extra pure dimethyl formamide (DMF), and ionic strength is maintained at 0.1 mol/L by using electrochemical grade tetrabutylammonium perchlorate (TBAP) as the supporting electrolyte. Solutions were deoxygenated by a stream of high purity nitrogen for 15 min prior to the experiments, and during the experiments nitrogen flow was maintained over the solution. 2,2-diphenyl-1-picrylhydrazyl radical (DPPH), ferrous chloride, α-tocopherol, 3-(2-pyridyl)-5,6-bis (4-phenyl-sulfonic acid)- 1,2,4-triazine (Ferrozine), ascorbic acid, ethylenediaminetetraacetic acid (EDTA), Trolox and dimethylformamide (DMF) were purchased from Sigma (Sigma–Aldrich GmbH, Sternheim, Germany). Methanol was purchased from E. Merck. Blank and standard antimicrobial susceptibility test discs were purchased from Oxoid. All other chemicals were analytical grade and obtained from either Sigma–Aldrich or Merck.

The 1,6-Bis(4-chloro-2-aminophenoxy)hexane used in the synthesis was prepared from 4-chloro-2-nitrophenole, 1,6-dibromohexane and K_2CO_3 as shown in Fig. 1 [33,34].

Synthesis of Schiff base

The 1,6-Bis(2-(5-bromo-2-hydroxybenzylideneamino)-4-chlorophenoxy)hexane was synthesized by the reaction of 5-bromosalicylaldehyde (40 mmol) with equivalent amount of 1,6-Bis(4-chloro-2-aminophenoxy) hexane (20 mmol) in ethanol medium. The reaction was continued for 2 h and the mixture cooled to room temperature, placed in a fridge for 24 h. Then the solid product was filtered, washed with cold ethanol and dried at 25 °C in a vacuum oven (Fig. 2).

Characterization of ligand (H_2L)

Molecular Weight: 735. m.p.: 168–170 °C. Color: Yellow. Yield: 12.28 g (83.6%). Anal Calcd. for $C_{32}H_{28}N_2O_4Cl_2Br_2$: C, 52.17, H, 3.81, N, 3.81. Found: C, 53.91, H, 4.17, N, 3.85. IR (cm^{-1}): 3071 υ(Ar—CH), 2915, 2871 υ(Alf.—CH), 1617 υ(C=N), 1492, 1469 υ(Ar—C=C), 1286, 1257 υ(Ar—O), 1173, 1162 υ(R—O). UV–vis: λ_1 = 264 nm(ε = 3500), λ_2 = 275(ε = 2900) nm λ_3 = 382 nm(ε = 3200). ^{13}C NMR (ppm, in DMSO-d_6): OCH_2CH_2: 26.72, OCH_2: 64.29, OH—C: 161.38, HC=N: 160.68, (Ar—C): 108.92, 113.56, 119.42, 120.06, 121.47, 121.52, 129.15, 134.12, 136.03 ^{1}H NMR (ppm, in DMSO-d_6): δ = 4.06 (t, OCH_2), δ = 1.75 (OCH_2CH_2, m), 1.52 ($OCH_2CH_2CH_2$, s) δ = 6.45–7.80 (Ar—H), δ = 8.95 (HC=N), δ = 13.64 (OH). Mass Spectra : *m/z:*735 $[H_2L]^+$.

Synthesis of Schiff base complexes

A solution of a metal salt such as Cu(II), Zn(II), Ni(II), Co(II) and V(III) in DMF (40 mL) was reacted with the Schiff base ligand (2 mmol) in DMF (60 mL) with 1:1 M ratio (Fig. 3). The content was refluxed for two hours on a hot plate-magnetic stirrer. The content was cooled to the room temperature, and solid product isolated by filtration, washed with cold ethyl alcohol and dried at 25 °C in a vacuum oven. The complexes yielded were not soluble in organic solvents besides dimethyl sulfoxide and dimethyl formamide.

Characterization of [CuL]

Molecular Weight: 797. m.p.: 202 °C decompose. Color: light brown. Yield: 1.23 g (77.4%). Anal Calcd. for $CuC_{32}H_{26}N_2O_4Cl_2Br_2$: C, 48.18, H, 3.26, N, 3.51 . Found: C, 49.02, H, 3.83, N, 3.48. Selected IR data (KBr, υ cm^{-1}): 3063 υ(Ar—CH), 2913, 2873 υ(Alf.—CH), 1607 υ(C=N), 1490, 1473 υ(Ar—C=C), 1233, 1197 υ(Ar—O), 1161, 1113 υ(R—O). λ_1 = 266 nm(ε = 12,100), λ_2 = 286 nm(ε = 9200),

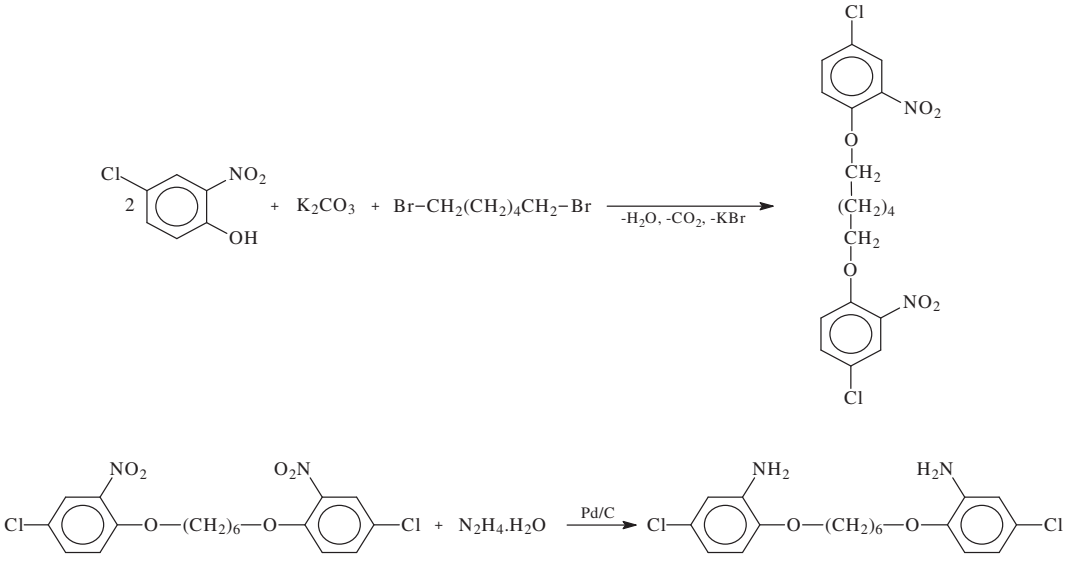

Fig. 1. Synthesis of the 1,6-Bis(4-chloro-2-aminophenoxy)hexane.

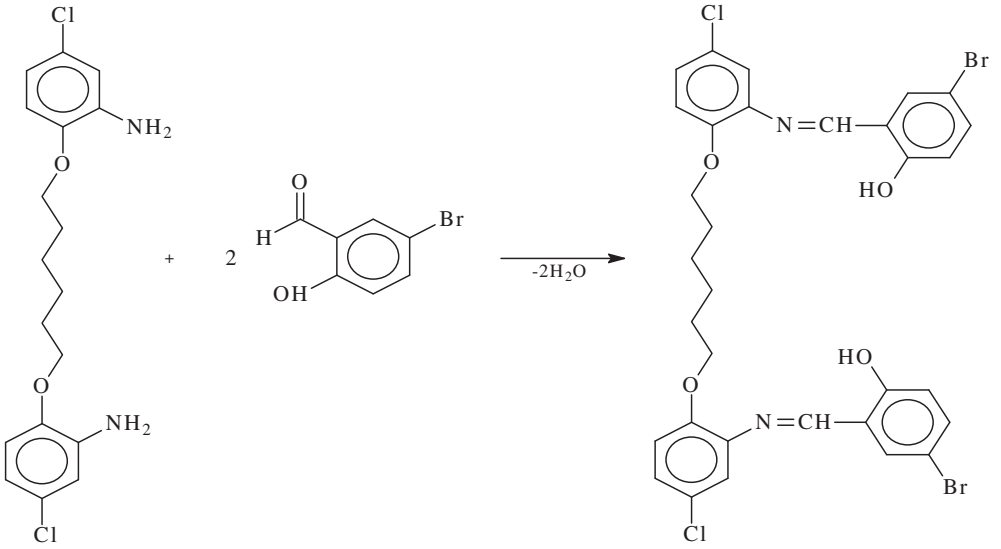

Fig. 2. Synthesis of the ligand (H_2L).

λ_3 = 394 nm(ε = 5600) μ_{eff} = 1.89 Bohr Magneton (B.M.) Mass Spectra : *m/z*:797 $[CuL]^+$.

Characterization of [NiL]

Molecular Weight: 791. m.p.: 110 °C decompose. Color: light brown. Yield: 1.14 g (72.2%). Anal Calcd. for $NiC_{32}H_{26}N_2O_4Cl_2Br_2$: C, 48.55, H, 3.28, N, 3.54. Found: C, 47.08, H, 3.30, N, 4.06. Selected IR data (KBr, υ cm^{-1})): 3066 υ(Ar—CH), 2929, 2857 υ(Alf.—CH), 1609, υ(C═N), 1488, 1450 υ(Ar—C═C), 1286, 1240 υ(Ar—O), 1159, 1187 υ(R—O). UV–vis (λmax, nm) in DMF: λ_1 = 260 nm(ε = 5000), λ_2 = 334 nm(ε = 1700), λ_3 = 430 nm(ε = 1500). μ_{eff} = 2.91 B.M. Mass Spectra : *m/z*:790 $[NiL–H]^+$.

Characterization of [CoL]

Molecular Weight: 792. m.p.: 157–160 °C. Color: Brown. Yield: 1.09 g (68.8%). Anal Calcd. for $CoC_{32}H_{26}N_2O_4Cl_2Br_2$: C, 48.48, H, 3.28, N, 3.54. Found: C, 50.15, H, 4.21, N, 3.97. Selected IR data (KBr, υ cm^{-1}): 3056 υ(Ar—CH), 2932, 2856 υ(Alf.—CH), 1610, υ(C═N), 1489, 1452 υ(Ar—C═C), 1285, 1248 υ(Ar—O), 1156, 1122 υ(R—O). UV–vis (λmax, nm) in DMF: λ_1 = 266 nm(ε = 3500), λ_2 = 352 nm(ε = 3200), λ_3 = 436 nm(ε = 960). μ_{eff} = 3.69 B.M. Mass Spectra : *m/z*:793 $[CoL + H]^+$.

Characterization of [ZnL]

Molecular Weight: 798. m.p.: 152–154 °C. Color: Orange. Yield: 1.05 g (66 %). Anal Calcd. for $ZnC_{32}H_{26}N_2O_4Cl_2Br_2$: C, 48.12, H, 3.26, N, 3.51. Found: C, 48.90, H, 4.22, N, 3.88. Selected IR data (KBr, υ cm^{-1}): 3070 υ(Ar—CH), 2947, 2857 υ(Alf.—CH), 1611, υ(C═N), 1491, 1459 υ(Ar—C═C), 1286, 1257 υ(Ar—O), 1174, 1160 υ(R—O). ^{1}H NMR (ppm): δ = 4.29 (OCH_2), δ = 6.92–7.96 (Ar—H), δ = 9.02 (HC═N). UV–vis (λmax, nm) in DMF: λ_1 = 259 nm(ε = 4300), λ_2 = 274 nm(ε = 3200), λ_3 = 361 nm(ε = 9600) λ_4 = 431 nm (ε = 1100). μ_{eff} = Diamagnetic. Mass Spectra : *m/z*:797 $[ZnL-H]^+$.

Characterization of [VLCl]

Molecular Weight: 820. m.p.: 167–170 °C. Color: Dark Brown. Yield: 0.95 g (58 %). Anal Calcd. for $VC_{32}H_{26}N_2O_4Cl_3Br_2$: C, 46.83, H, 3.17 , N, 3.41 . Found: C, 47.22, H, 4.10, N, 3.97. Selected IR data

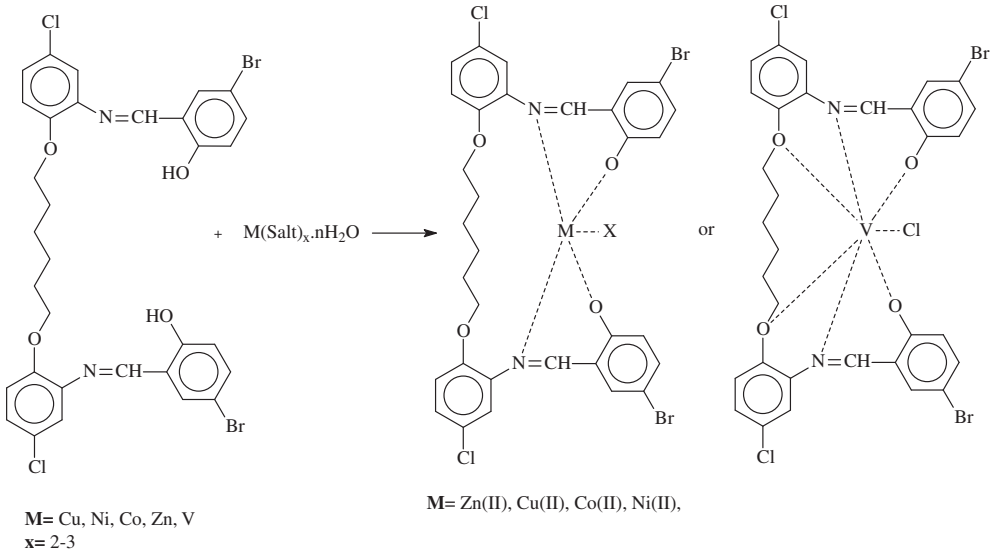

Fig. 3. Synthesis of the complexes.

(KBr, υ cm^{-1}): 3069 υ(Ar—CH), 2940, 2859 υ(Alf.—CH), 1611, υ(C=N), 1491, 1471 υ(Ar—C=C), 1281, 1253 υ(Ar—O), 1126, 1173 υ(R—O). UV–vis (λmax, nm) in DMF: λ_1 = 262 nm(ε = 3300), λ_2 = 362 nm(ε = 3320). μ_{eff} = 2.84 B.M. Mass Spectra : *m/z*:822 $[VLCl + 2H]^+$.

Antioxidant analyses of the compounds

DPPH scavenging activity

Free radical scavenging capacities of the complexes were determined by previously reported procedure using the stable 2,2-diphenyl-1-picrylhydrazyl radical (DPPH) [35]. The solutions of the compounds (0.1 mL) at different concentrations (5, 10, 25, 50 and 100 mg/L) were added to 3.9 mL of freshly prepared DPPH in methanol. The mixture was shaken and stands for 30 min in the dark at room temperature. Finally the absorbance were measured at 517 nm against a blank solution which consist 4 mL methanol. Ascorbic acid and Trolox were used as positive control to compare the activities. The formula of DPPH scavenging activity is;

$$I\% = (A_{control} - A_{sample})/A_{control} \times 100;$$

where $A_{control}$ is the absorbance of the control reaction (containing all reagents except the test compound), and A_{sample} is the absorbance of the test compound. Tests were carried out in triplicate. Trolox and ascorbic acid were used as positive control.

Chelating effects on ferrous ions

Metal chelating effects on ferrous ions exhibited by the compounds was carried out as described by Hsu et al. [36] 1 mL of the synthesized compounds solutions (DMF) at varied concentrations, 0.1 mL 2 mM $FeCl_2.H_2O$, 0.2 mL 5 mM ferrozine-1,2,4-triazine (Sigma) and 3.7 mL methanol were mixed in a test tube and reacted for 10 min. The absorbance of reactants was measured at 562 nm. The mixture without extract was used as control. A lower absorbance indicates a higher ferrous ion chelating capacity and was check against EDTA (Sigma) as a positive control using formula below;

$$\text{Metal chelating effect} : (A_{control} - A_{sample})/A_{control} \times 100$$

where $A_{control}$ is the absorbance of the control reaction (containing only $FeCl_2$ and ferrozine), and A_{sample} is the absorbance of the compounds/reference. EDTA was used as a positive control.

Antimicrobial analyses

In vitro antibacterial studies were done for determining the antimicrobial potentials of the compounds used in this study. For this purpose disc diffusion method was used [37]. *Escherichia coli* (ATCC 10536), *Staphylococcus aureus* (ATCC 6538), *Bacillus subtilis* (6051) Legionella pneumophila subsp. *pneumophiia* (ATCC 33152), *Enterococcus hirae* (ATCC 10541), *Micrococcus luteus* (ATCC 9341), and *Pseudomonas aeruginosa* (ATCC 9027) were used as test microorganisms. Bacterial cultures were incubated at 37 °C for 24 h in Nutrient Broth. Each plate was filled with 25 mL of Nutrient Agar. 100 μL of the bacteria culture suspension inoculated to petri plates and dealt with a drigalski spatula. The blank discs (6.0 mm, Oxoid Ltd, Wade Road, Basingstoke, Hants, RG24 8PW, UK.) were impregnated with 15 μL compound solutions. Same volume (15 μL) of DMF was used as control. The inoculated plates were incubated for 24 h. The diameters of the inhibition zones were measured with calipers.

Results and discussion

Schiff base and complexes

In this work, we have synthesized a new Schiff-base ligand and its some metal complexes. The ligand and metal complexes were characterized by elemental analysis, IR, UV–vis, TGA-DTA, ^{1}H NMR and ^{13}C NMR, conductivity measurements, cyclic voltammetry and magnetic susceptibility studies. Some theoretical computations such as optimization, ^{1}H NMR, frontier orbitals (Highest Occupied Molecular Orbital (HOMO) and Lowest Unoccupied Molecular Orbital (LUMO)) visualization studies were also carried out as supportive characterizations for the ligand. Additionally a linear regression analysis was also done to determine the compatibility between theoretical and experimental ^{1}H NMR shifts.

FTIR spectra

Some characteristic IR bands/peaks of the compounds can be seen in Table 1. Due to the strong intramolecular interactions between hydroxyl groups and imine groups in the ligand, hydroxyl (O—H) stretching band/peak could not be observed in the region expected (~3300 cm^{-1}). In the literature there are many papers that explains the intramolecular hydrogen bonding [38,39]. The

FT-IR spectra of the aldehyde and amine showed the IR bands at 1735 and 3420 cm^{-1} due to υ(C=O) and υ(NH_2) stretching vibrations disappeared and instead, in the IR spectra of the ligand a new band was observed 1617 cm^{-1} attributed to azomethine υ(C=N) group. This finding/change suggests that the amino and aldehyde groups of the starting reactants have been converted into the corresponding Schiff base. The peak at ~1285 cm^{-1} in the IR spectrum of the ligand is assigned to the phenolic C—O stretching vibration. This peak is found in a region lower than ~1285 cm^{-1} in the spectra of the metal complexes. The peaks around 1610 cm^{-1} in FT-IR of the complexes can be assigned to stretching vibrations of azomethine υ(—C=N) groups [40–42]. The stretching vibrations of azomethine υ(—C=N) groups in the complexes were shifted to lower values. It is assumed that these shifts to the lower values are the proofs for the coordination between C=N groups and metals [43]. In the spectra of the compounds the bands at 2965–2855 cm^{-1} are assigned to υ(Aliphatic C—H) groups and 3050–3100 cm^{-1} υ(Aromatic C—H) stretching vibrations [44].

Electronic spectra

The ultraviolet–visible (UV–vis) spectral data (in DMF) of the compounds at room temperature can be found in experimental section. The electronic spectra of the compounds showed few bands in the UV–vis region (200–900 nm). The absorption bands below at ca.300 nm are practically identical and can be assigned to $\pi \rightarrow \pi^*$ transitions in the benzene ring and azomethine (—C=N) groups. The absorption bands observed within the ca. 300–400 nm range are due to the $n \rightarrow \pi^*$ transitions in imine and phenoxy groups of the ligand and its metal complexes [45].The transitions such as $n \rightarrow \pi^*$ and $\pi \rightarrow \pi^*$ in the ligand were shifted to higher wavelengths in the complexes [46]. These changes are the signs the formation of the coordination between metal and ligand [45,46].

Magnetic measurements and molar conductivity

The magnetic moments of the complexes were measured room temperature. The measurements give additional information for characterization of the complexes. The magnetic moment values of the complexes can be found in the characterization section. It was determined that all the complexes are non-electrolytes. The molar conductivity values of the complexes (in DMF) are in the range reported for non-electrolytes [47–49].

^{1}H NMR and ^{13}C NMR

The ^{1}H NMR and ^{13}C NMR spectra of the ligand and its Zn(II) complex were recorded (solvent, DMSO-d_6). The interpretations of those spectra are given in the experimental section. Structural information about the ligand was provided by ^{13}C NMR spectra in details. All of the aliphatic, aromatic and azomethine carbon (CH=N) shifts were confirmed in the regions expected [50]. The phenolic protons' signals were not observed in the ^{1}H NMR spectra of the Zn(II) complex. Those signals were observed in the ^{1}H NMR spectra of the ligand. The elimination of the phenolic protons or the absence of phenolic proton signal proofs the formation of the [ZnL] complex. In the ^{1}H NMR spectra of [ZnL] complex imine group's proton (—CH=N—) showed a higher value than the ligand's imine group. This is another proof for the formation of [ZnL] complex [51].

TGA studies

The thermal stabilities of the compounds were confirmed by thermal gravimetric analyses. The termogravimetric analyses (TGA) are given in Table 2 and the thermograms were obtained at a heating rate of 10 °C/min in a nitrogen atmosphere over a temperature range of 50–900 °C. [29,31]. The detailed information about thermal stabilities, decompositions can be found in Table 2.

Mass spectra

The mass spectra of the complexes peaks attributable to the molecular ions *m/z*: 735 $[H_2L]^+$, *m/z*: 797 $[CuL]^+$, *m/z*: 790 $[NiL-H]^+$, *m/z*: 793 $[CoL + H]^+$, *m/z*: 797 $[ZnL-H]^+$, *m/z*: 822 $[VLCl + 2H]^+$.

Theoretical studies

Structure optimization [52] carried out by applying B3LYP level of Density Functional Theory (DFT) [53] at the 6-311G basis set. Optimized 3D structure of the ligand can be seen in Fig. 4. NMR calculations [54] carried out by applying DFT and Hartree Fock (HF) [55] theories with different levels and basis sets (Fig. 5 and Table 3). In this study, Gauge-Independent Atomic Orbital (GIAO) method was applied to compute theoretical NMR shifts of the ligand, at gas phase [56–60].

Frontier orbitals (Highest Occupied Molecular Orbital (HOMO) and Lowest Unoccupied Molecular Orbital (LUMO)) and transition energy levels are shown in Fig. 6. Frontier molecular orbitals energies were computed at B3LYP/6-311G level of the DFT method [61]. The difference of the energy level between HOMO and LUMO orbitals can be also seen in Fig. 6. The energy levels of HOMO and LUMO structures were found −6.1918 eV and −2.5752 eV respectively. The excitation energy value for the HOMO–LUMO transition was found as 3.6166 eV and, this energy value can be assigned to the $\pi \rightarrow \pi^*$ transition in the aromatic rings and C=N groups (Fig. 6). Formation of π bonds can be clearly seen in Fig. 6 by the interaction of p orbitals, in the HOMO view.

On the other hand, a linear regression analysis was also done to control the compatibility between experimental and theoretical ^{1}H NMR shifts of the ligand, as a supportive characterization technique to the experimental characterization techniques. Regression analysis data of the theoretical and experimental NMR shifts can be seen in Table 4. The table shows the comparison of experimental data to theoretical Hartree–Fock and B3LYP methods' data. Although outlier, being the most extreme observations, can have many anomalous causes, its exclusion can make the model meth-

Table 1
Physical characterization, analytical, molar conductance and spectral data of the compounds.

Compound	Yield (%)	Color	Melting point (°C)	Formula weight	(Calcd.) Found %C	%H	%N	ν(C=N) (cm^{-1})	μ_{eff} (BM)
Ligand (H_2L)	12.28 (83.6)	Yellow	168–170	735	(52.17) 53.91	(3.81) 4.17	(3.81) 3.85	1617 m	–
[CuL]	1.23 (77.4)	Light Brown	202 Decom.	797	(48.18) 49.02	(3.26) 3.83	(3.51) 3.48	1607 m	1.89
[NiL]	1.14 (72.2)	Light Brown	110 Decom.	791	(48.55) 47.08	(3.28) 3.30	(3.54) 4.06	1609 m	2.91
[CoL]	1.09 (68.8)	Brown	157–160	792	(48.48) 50.15	(3.28) 4.21	(3.54) 3.97	1610 m	3.69
[ZnL]	1.05 (66)	Orange	152–154	798	(48.12) 48.90	(3.26) 4.22	(3.51) 3.88	1611 m	–
[VLCl]	0.95 (58)	Dark Brown	167–170	820	(46.83) 47.22	(3.17) 4.10	(3.41) 3.97	1611 m	2.84

m : medium.

Table 2
TGA data of the complexes.

Compounds	First Step, °C (DTG °C) Weight loss %, Calculated (Found) Decomposition group	Second Step, °C(DTG °C) Weight loss %, Calculated (Found) Decomposition group	Third Step, °C (DTG °C) Weight loss %, Calculated (Found) Decomposition group
Ligand (H_2L)	290–365 (324) 42.2 (41.3) $C_{12}H_6Br_2$	365–615 (531) 67.6 (69.1) $C_6H_{12}O_2$ and Cl_2	
[CuL]	260–380 (323) 53.4 (54.0) $C_{12}H_6Br_2$	380–756 (462) 90.1 (89.5) Residue CuO	
[NiL]	287–376 (326) 19.6 (20.5) C_6H_3Br	376–608 (566) 53.9 (54.1) C_6H_3Br and $C_6H_{12}O_2$	608–805 (674) 90.6 (90.0) Residue NiO
[CoL]	298–332 (330) 19.6 (20.0) C_6H_3Br	332–481 (453) 53.8 (53.1) C_6H_3Br and $C_6H_{12}O_2$	481–684 (616) 90.7 (90.0) Residue CoO
[ZnL]	316–355 (350) 19.5 (20.1) C_6H_3Br	355–491 (420) 53.4 (55.2) C_6H_3Br and $C_6H_{12}O_2$	491–808 (695) 89.7 (89.8) Residue ZnO
[VLCl]	264–311 (305) 18.9 (21.3) C_6H_3Br	311–452 (420) 51.9 (53.2) C_6H_3Br and $C_6H_{12}O_2$	

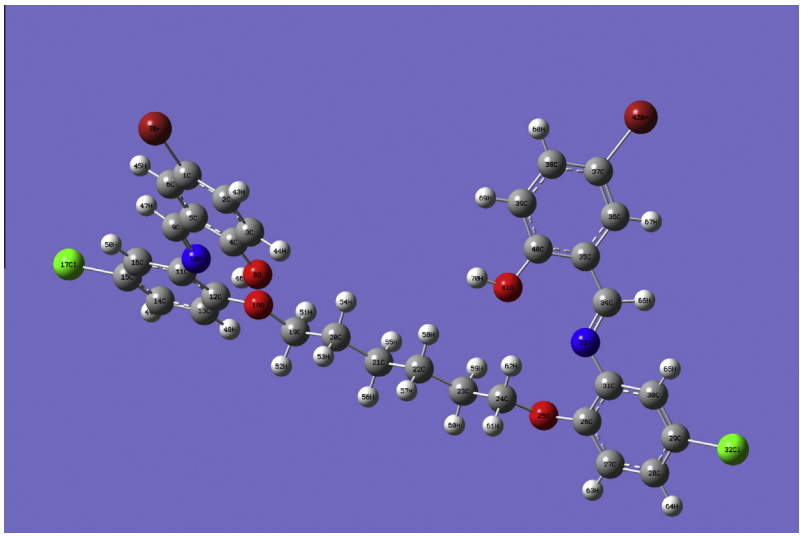

Fig. 4. Optimized 3D structure of the ligand (H_2L) (B3LYP/6-311G).

odologically sounds. The *R*-Squared statistic indicates that the models as fitted explain 70.7% included outlier, but 93.2% without outlier of the variability in experimental data. Moreover the correlation coefficient equals 0.841 and 0.965 for the model with outlier and without outlier respectively, indicating a shift from a moderately strong relationship to strong relationship between the variables. Finally, the estimated standard error shows the standard deviation of the residuals to be 1.947 for the model with outlier, and 0.860 for model without outlier. This value can be used to construct prediction limits for new observations.

According to the regression analysis, there is a good conformity between experimental and theoretical ^{1}H NMR shifts (Fig. 5 and Table 3) but only the values for phenolic protons' (the proton numbered 70) experimental NMR shifts (13.6437) are very different (Table 3) than theoretical (HF = 4.0769 and B3LYP = 3.3614) because of this difference, estimated standard error is higher than expected. If the values for the 70 numbered protons neglected then a very high accuracy regression results are obtained (Table 4). The change and difference between theoretical and experimental NMR shifts can be assigned to acidic character of phenolic protons and executing theoretical calculations in the gas phase [62–64].

Electrochemical analysis

The CV technique (on a glassy carbon electrode in DMF containing 0.1 M TBAP, in the concentration of 1×10^{-3} M vs. Ag/AgCl) was applied to investigate the electrochemical properties of the compounds. The electrochemical data is presented in Table 5. The oxidation potentials can be measured by cyclic voltammetry and then the HOMO and LUMO values are calculable [65]. The corresponding HOMO and LUMO levels were calculated using IVc and IIa waves for the L ligand. The estimations were done with the empirical relation $E_{LUMO} = [(E_{IVc} - E_{1/2}(\text{ferrocene})) + 4.8]$ eV or $E_{HOMO} = [(E_{IIa} - E_{1/2}(\text{ferrocene})) + 4.8]$ eV. Ferrocene was used as external standard. It shows two peaks at 0.34 and 0.40 V hence the $E_{1/2}$ (ferrocence) is equal to 0.37 V which can be used in equa-

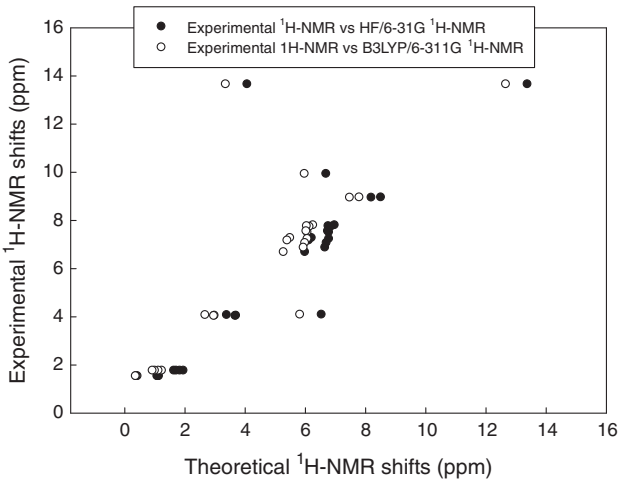

Fig. 5. The scatter plot for the compatibility of experimental and theoretical ^{1}H NMR shifts (for the ligand).

tion to calculate the E_{HOMO} and E_{LUMO}. Based on cyclic voltammetry results, Ligand (L) shows E_{HOMO} = 5.11 eV, Egap = 1.96 eV and E_{LUMO} = 2.48 eV.

In the cathodic direction from +1.0 V to −2.3 V at scan rate of 100 mV s^{-1}, the CV of L is characterized by four cathodic waves (Ic, IIc, IIIc and IVc at about −0.25 V, −0.48, −1.68 and −1.95 V respectively) and two waves were observed (Ia and IIa at about +0.12 V and +0.68 V respectively) as depicted by cyclic voltammograms given in Fig. 7(A). At high scanning rates (200 mV/s>), IIa peak was not observed (Fig. 8(A)).

In Fig. 7(B), the voltammogram taken at in the reduction direction of CuL complex in 1×10^{-3} concentration, at the potential range of −2.3 V and +1.0 V, at 100 mV/s scan rate is seen. The CV of CuL was characterized by a cathodic peak (Ic at about −1.28 V) and three anodic waves (Ia, IIa and IIIa t about −1.05 V, −0.30 V and +0.48 V). ΔE_p for Ia/Ic for this redox couple was also found as 230 mV. This is the sign of a quasi-reversible electron transfer in the electrode reaction. It should be taken in consideration [66–68] that after occurring the one-electron reduction process corresponding to [Cu^{II}L]/[Cu^{I}L], part of [Cu^{I}L] species are chemically decomposed to copper metal (reaction 1). So, it can be said that the corresponding anodic waves (IIa and IIIa) are related to the re-oxidation of electrodeposited copper metal to free Cu^+/Cu^{2+} according to the reaction 2:

$$[Cu^{II}L] \leftrightarrow Cu^{+2} + L + e^- \leftrightarrow Cu^+ + L \quad (1)$$

$$Cu^+ \leftrightarrow Cu^{+2} + e^- \quad (2)$$

The effect of scan rates on CuL complex was investigated between the 50–1000 mV/s (Fig. 8(B)). At high scan rate (200 mV/s>), The IIa peak was not observed (Fig. 9(B)).

The voltammograms of NiL complex investigated in the same experimental conditions (from +1.0 V to −2.3 V at 100 mV s^{-1} in (Fig. 7(C)), two waves (Ic and IIc at about −0.78 and −1.81 V, respectively) and two anodic waves (Ia and IIa at about −1.71, and +0.45 V, respectively). The effect of scan rates on NiL complex was investigated between 50 and 100 mV/s (Fig. 8(C)).

In the potential range of −2.3 V to +1.0 V at scan rate of 100 mV s^{-1}, on the cathodic side, the CV of CoL complex (Fig. 7(D)) shows two cathodic peaks (Ic and IIc at about −0.73 and −1.12 V, respectively) and one anodic peak ((Ia at about +0.39 V). Of these, Ic oxidation step seems to be weak.

From the CVs (Fig. 7), it was found that the initial oxidation peak current of L, CuL, NiL and CoL progressively increased and a negative shift in the peak potentials existed with increasing scan rate. From the results obtained between 50 and 1000 mV s^{-1}, a plot of logarithm of peak current significantly correlated with the logarithm of scan rate for all L, CuL, NiL and CoL with slopes between 0.43, 0,47, 0.49 and 0.50, respectively (correlation coefficient between 0.986, 0.957, 0.969 and 0.949). These results show that the redox processes were predominantly diffusion controlled in

Table 3
Comparison of the experimental and theoretical ^{1}H NMR shifts.

Nuclei	^{1}H NMR Experimental (ppm)	^{1}H NMR HF/6-31G (d) (ppm)	Error	^{1}H NMR B3LYP/6-311G (2d,p) (ppm)	Error
46-H	13.6437	13.3856	0.258	12.6701	0.973
47-H	8.9501	8.5169	0.433	7.8014	1.148
66-H	8.9385	8.1988	0.739	7.4833	1.455
67-H	7.7944	6.9815	0.812	6.2660	1.528
43-H	7.7298	6.8610	0.868	6.1455	1.584
50-H	7.4977	6.7919	0.705	6.0764	1.421
63-H	7.2226	6.7911	0.431	6.0756	1.147
45-H	7.7561	6.7697	0.986	6.0542	1.701
68-H	7.5458	6.7511	0.794	6.0356	1.510
64-H	7.0540	6.7108	0.343	5.9953	1.058
49-H	9.9231	6.6984	3.224	5.9829	3.940
44-H	6.8604	6.6630	0.197	5.9475	0.912
62-H	4.0788	6.5456	−2.466	5.8301	−1.751
65-H	7.2655	6.2158	1.049	5.5003	1.765
48-H	7.1616	6.1233	1.038	5.4078	1.753
69-H	6.6756	5.9982	0.677	5.2827	1.392
70-H	13.6437	4.0769	9.566	3.3614	10.282
52-H	4.0393	3.7051	0.334	2.9896	1.049
51-H	4.0243	3.6833	0.341	2.9678	1.056
61-H	4.0636	3.3950	0.668	2.6795	1.384
53-H	1.7547	1.9551	−0.200	1.2396	0.515
54-H	1.7547	1.8423	−0.087	1.1268	0.627
60-H	1.7547	1.7227	0.032	1.0072	0.747
59-H	1.7547	1.6431	0.111	0.9276	0.827
57-H	1.5235	1.144	0.379	0.4285	1.095
56-H	1.5235	1.1129	0.410	0.3974	1.126
58-H	1.5235	1.1111	0.412	0.3956	1.127
55-H	1.5235	1.0841	0.439	0.3686	1.154

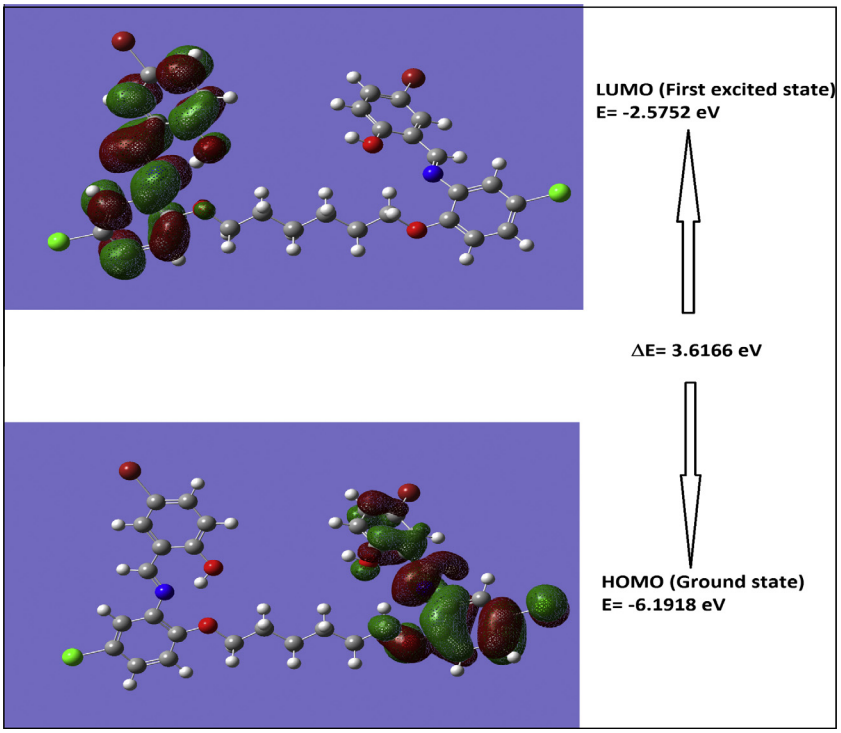

Fig. 6. Mesh view of the frontier orbitals (HOMO–LUMO) of the ligand and the energy levels (for the ligand).

Table 4
Regression analysis data of the theoretical and experimental ^{1}H NMR shifts.

Compared methods	B	M	*R*-squared	Standard error	Correlation coefficient
Experimental vs. HF	0.773	1.005	0.707	1.947	0.841
Experimental vs. B3LYP	1.493	1.005	0.707	1.947	0.841
Experimental vs. HF[a]	0.247	1.045	0.932	0.860	0.965
Experimental vs. B3LYP[a]	0.995	1.045	0.932	0.860	0.965

[a] Without outlier.

Table 5
Voltammetric results at scan rate of 100 mV s^{-1} vs. Ag/AgCl. Ec: cathodic potential, Ea: anodic potential.

Compound	Ec (V)	Ea (V)
H_2L	Ic: −0.25, IIc: −0.48, IIIc: −1.68 IVc: −1.95	Ia: +0.12, IIa: +0.68
CuL	Ic: −1.28	Ia: −1.05, IIa: −0.30, IIIa: +0.48
NiL	Ic: −0.78, IIc: −1.81	Ia: −1.71, IIa: +0.45
CoL	Ic: −0.73, IIc: −1.12	Ia: +0.39

the whole scan rates range studied. Voltammetric results are presented in Table 5.

Antioxidant and antimicrobial studies

DPPH scavenging activity

In this study, the antioxidant activity of the DMF solutions of the five compounds was studied using the DPPH scavenging assay. In DPPH scavenging activity different concentrations of compounds were studied (5, 10, 25, 50 and 100 mg/L). The antioxidant activities of the compounds were increased with concentration as seen in Fig. 9. The highest activity was exhibited by V(III) as 49.29% this is followed by Zn(II) as 38.41% , ligand as 32.15%, Ni(II) as 30.37%, Co(II) as 25.53% and Cu(II) as 25.29%. The standard antioxidants used in this study showed excellent activity as 99.05 % by ascorbic acid and as 98.58 % by trolox. In this study almost the same results with Agırtas et al. were obtained [69,70].

Metal chelating and antibacterial activity

In the study of metal chelating activity studied compounds were executed quite high antioxidant activity as shown in Fig. 10. Especially ligand showed high activities even at low concentrations. The chelating activities of compounds at 100 mg/L concentration were 97.31% for ligand, 90.10% for V(III), 89.48% for Zn(II), 88.65% for Ni(II), 84.53% for Cu(II) and 66.80% for Co(II). EDTA showed slightly higher activity than ligand. From this point of view ligand may be used alternatively at the applications that EDTA was used. Some chemical modifications may make ligand more powerful than EDTA. For this reason further laboratory studies should be done. The metal chelating activity findings are better than the study of Agirtas et al. [69,70].

Compounds were analyzed for their antibacterial activities as seen in Table 6. According to the results obtained from the study some results were not reliable; except Cu(II), all the compounds showed slightly weak activity against *B. subtilis*. Ni(II) showed the highest antibacterial activity as 24 mm against *E. coli*. This activity is higher than the amikacin and equal to tetracycline. Amongst the compounds V(III) was exhibited antibacterial activity only against *E. hirae* as 13 mm. Only Ni(II) exhibited antibacterial activity against to all bacteria. All the compounds tested in this study showed antimicrobial activity against *E. hirae*. Amikacin and tetracycline displayed excellent activity against to test bacteria

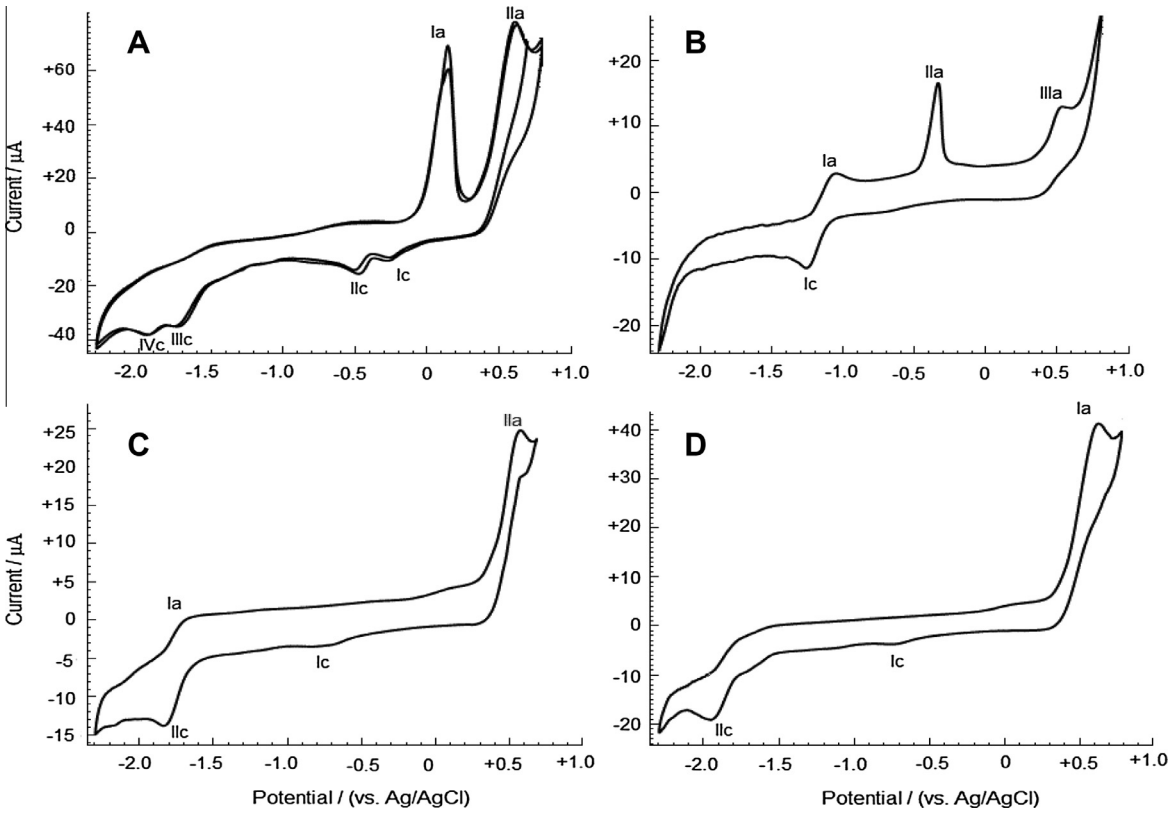

Fig. 7. Cyclic voltammograms of 1×10^{-3} mol L^{-1} compound solutions in DMF at glassy carbon electrode; (A) **L**, (B) **CuL**, (C) **NiL**, (D) **CoL** scan rate, v: 100 mV s^{-1}.

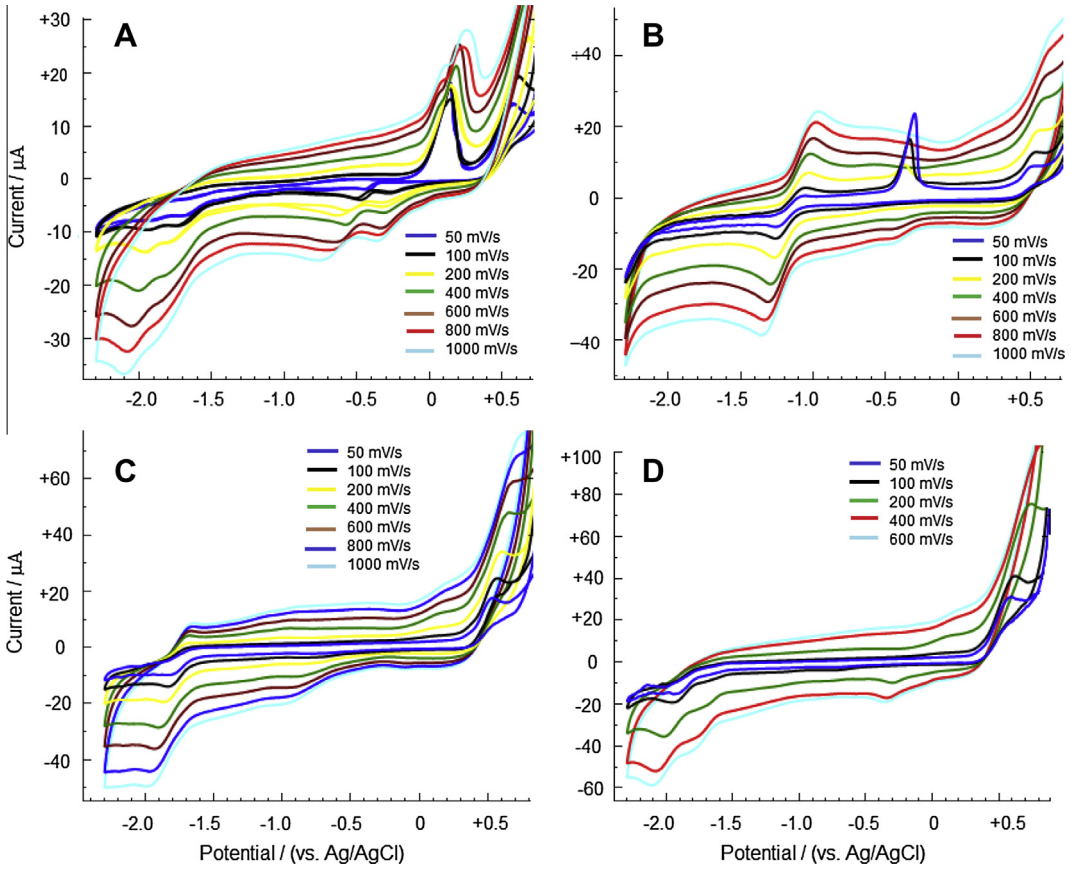

Fig. 8. Cyclic voltammograms of 1×10^{-3} mol L^{-1} compound solutions at different scan rates; (A) **L**, (B) **CuL**, (C) **NiL**, (D) **CoL**.

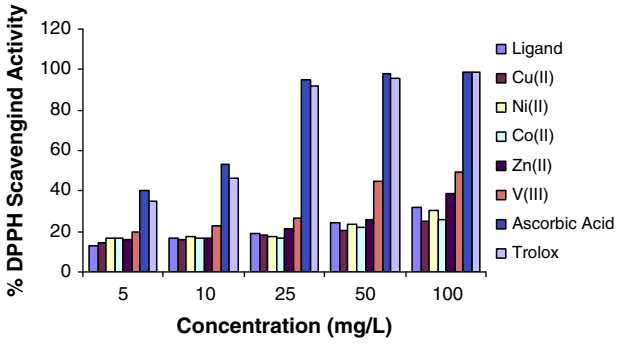

Fig. 9. DPPH scavenging activity of different concentrations of Schiff base and its metal complexes.

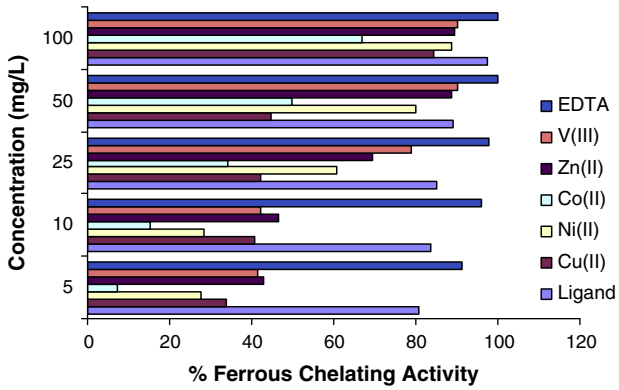

Fig. 10. Metal chelating activity of Schiff base and its metal complexes.

Table 6
Antibacterial activity of compounds and standard antibiotics.

Bacteria	Compounds and antibiotic discs[a]							
	L	Cu(II)	Ni(II)	Co(II)	Zn(II)	V(III)	AK	TE
P. aeriginosa	0	0	11	8	0	0	21	24
S. aureus	7	8	10	0	0	0	24	32
L. pneumophila subsp pneumophiia	8	10	8	0	8	10	16	20
B. subtilis	7	0	8	8	9	10	20	23
M. luteus	8	7	12	0	9	8	18	24
E. hirae	10	12	10	9	7	13	21	18
E. coli	0	0	24	8	10	12	23	24

[a] Inhibition diameter in millimeters. H_2L = Ligand, AK = Amikacin (30 μg), TE = Tetracycline (30 μg).

compared to the compounds. The highest antimicrobial activity exhibited by tetracycline against *S. aureus* as 32 mm amongst the compounds and standard antibiotics.

Conclusion

Five metal complexes of a new Schiff base were synthesized and characterized. The suggested structures of the complexes are presented in Figs. 2 and 3. According to the findings, [NiL], [CoL], [ZnL] complexes may have tetrahedral and [CuL] complex may have square planar structures. V(III) may have the following geometries such as complex may show a capped octahedron in which a seventh ligand have been added to triangular face around the central metal ion [71–77]. Antimicrobial activity of the compounds (DMF solutions) possessed intermediate antibacterial activity compared to the amikacin and tetracycline. Especially Ni(II) effected all the microorganisms studied. Some modifications of Ni(II) complex may have more effect against to bacteria. The antioxidant activity of the compounds on DPPH scavenging and metal chelating activity were concentration dependent. The compounds exhibited moderate DPPH scavenging activity compared to the standards. Excellent metal chelating activities were exhibited by the compounds. Particularly ligand showed almost about 100% chelating activity.

Acknowledgements

This study was supported by Scientific Research Projects Unit of Siirt University (Project code: BAP- 2011-SİÜFED-YL1), (Turkey).

Appendix A. Supplementary material

Supplementary data associated with this article can be found, in the online version, at http://dx.doi.org/10.1016/j.molstruc.2014.06.062.

References

[1] A.M. Vijesh, A.M. Isloor, P. Shetty, S. Sundershan, H.K. Fun, Eur. J. Med. Chem. 62 (2013) 410–415.
[2] J. Patole, D. Shingnapurkar, S. Padhye, C. Ratledge, Bioorg. Med. Che. Let. 16 (2006) 1514–1517.
[3] B.S. Holla, B. Veerendra, M.K. Shivananda, B. Poojary, Eur. J. Med. Chem. 38 (2003) 759–767.
[4] K.V. Sujith, J.N. Rao, P. Shtty, B. Kalluraya, Eur. J. Med. Chem. 44 (2009) 3697–3702.
[5] S.A. Hayta, M. Arisoy, O.T. Arpaci, İ. Yıldız, E. Aki, S. Özkan, F. Kaynak, Eur. J. Med. Chem. 43 (11) (2008) 2568–2578.
[6] A.M. Isloor, B. Kalluraya, P. Shetty, Eur. J. Med. Chem. 44 (2009) 3784–3787.
[7] M. Verma, S.N. Pandeya, K.N. Singh, J.P. Stables, Acta Pharm. 54 (2004) 49–56.
[8] A.K. Singh, V.K. Gupta, B. Gupta, Anal. Chim. Acta 585 (2007) 171–178.
[9] E.M. Hodnett, W.J. Dunn, J. Med. Chem. 15 (1972) 339–344.
[10] B. Tozkoparan, E. Kupeli, E. Yesilada, M. Ertan, Bioorg. Med. Chem. 15 (2007) 1808–1814.
[11] E.M. Hodnett, W.J. Dunn, J. Med. Chem. 13 (1970) 768–770.
[12] M.S. Karthikeyan, D.J. Prasad, B. Poojary, K.S. Bhatt, B.S. Holla, N.S. Kumari, Bioorg. Med. Chem. 14 (2006) 7482–7489.
[13] J. Abildgaard, P.E. Hansen, J. Josephsen, B.K.V. Hansen, H.O. Sorensen, S. Larsen, Inorg. Chim. Acta. 359 (2006) 4493–4502.
[14] P. Panneerselvam, R.R. Nair, G. Vijayalakshmi, E.H. Subramanian, S.K. Sridhar, Eur. J. Med. Chem. 40 (2005) 225–229.
[15] S.N. Pandeya, D. Sriram, G. Nathand, E. De Clercq, Eur. J. Pharm. Sci. 9 (1999) 25–31.
[16] S.N. Pandeya, D. Sriram, G. Nath, E. De Clercq, Pharm. Acta, Helv. 74 (1999) 11–17.
[17] U. Demirbas, R. Bayrak, M. Piskin, H.T. Akcay, M. Durmus, H. Kantekini, J. Organomet. Chem. 724 (2013) 225–237.
[18] K. Singh, M.S. Barwaand, P. Tyagi, Eur. J. Med. Chem. 41 (2006) 147–153.
[19] H. Keypour, H. Khanmohammadi, K.P. Wainwrightand, M.R. Taylor, Inorg. Chim. Acta 357 (2004) 1283–1291.
[20] G.B. Bagihalli, P.G. Avaji, S.A. Patil, P.S. Badami, Eur. J. Med. Chem. 43 (2008) 2639–2649.
[21] T.W. Hambley, L.F. Lindoy, J.R. Reimers, P. Turner, W. Wei, A.N.W. Copper, J. Chem. Soc. Dalton Trans. 5 (2001) 614–620.
[22] S. Chandra, L.K. Gupta, Trans. Met. Chem. 30 (2007) 630–635.
[23] T.M.A. Ismail, J. Coord. Chem. 58 (2005) 141–151.
[24] P.R. Fenton, R. Gauci, P.C. Junk, L.F. Lindoy, R.C. Luckay, G.V. Meehan, J.R. Price, P. Tumer, G. Wei, J. Chem. Soc. Dalton Trans. (2002) 2185–2193.
[25] T.M.A. Ismail, A.A. Saleh, M.A. El Ghamry, Spectrochim. Acta, Part A 86 (2012) 276–288.
[26] E. Tas, A. Kilic, M. Durgun, L. Küpercik, I. Yilmaz, S. Arslan, Spectrochim. Acta Part A. 75 (2010) 811–818.

[27] D. Arish, M.S. Nair, Arabian J. Chem. 5 (2012) 179–186.
[28] H. Temel, H. Alp, S. Ilhan, B. Ziyadanoğulları, I. Yilmaz, Monatsh. Chem. 138 (2007) 1199–1209.
[29] S. Ilhan, H. Temel, I. Yilmaz, M. Sekerci, J. Organomet. Chem. 692 (2007) 3855–3865.
[30] S. Ilhan, H. Temel, I. Yilmaz, M. Sekerci, Polyhedron 26 (2007) 2795–2802.
[31] C.R. Bhattacharjee, P. Goswami, P. Mondal, Inorg. Chim. Acta 387 (2012) 86–92.
[32] A. Earnshaw, Introduction to Magnetochemistry, Acedemic Press, London, 1968.
[33] S. Ilhan, J. Coord. Chem. 61 (2008) 3634–3641.
[34] H. Temel, S. Ilhan, Russ. J. Coord. Chem. 33 (2007) 918–991.
[35] S.V. Jovanovic, S. Steenken, M. Tosic, B. Marjanovic, M.G. Simic, Am. J. Chem. Soc. 116 (1994) 4846–4851.
[36] C. Hsu, W. Chen, Y. Weng, C. Tseng, Food Chem. 83 (2003) 85–92.
[37] D. Kalemba, A. Kunicka, Curr. Med. Chem. 10 (2003) 813–829.
[38] H. Temel, S. Ilhan, M. Şekerci, R. Ziyadanogulları, Spect. Lett. 35 (2002) 219–228.
[39] S. Ilhan, H. Temel, A. Kılıç, Chinese J. Chem. 25 (2007) 1–10.
[40] S. Ilhan, H. Temel, Trans. Met. Chem. 32 (2007) 1039–1046.
[41] S. Ilhan, H. Temel, A. Kılıç, I. Yılmaz, Trans. Met. Chem. 32 (2007) 344–349.
[42] H. Temel, S. Ilhan, M. Aslanoglu, A. Kilic, E. Tas, J. Chin. Chem. Soc. 53 (2006) 1027–1031.
[43] A.A. Saleh, J. Coord. Chem. 58 (2005) 255–270.
[44] H. Temel, S. Ilhan, Spectrochim. Acta, Part A 69 (2008) 896–903.
[45] I. Yılmaz, S. Ilhan, H. Temel, A. Kılıc, J. Inc. Phenom. Macrocyclic Chem. 63 (2009) 163–169.
[46] S. Ilhan, H. Temel, M. Sünkür, I. Tegin, Indian J. Chemi. Sec A. 47A (2008) 560–564.
[47] S. Ilhan, J. Chem. Res. 1 (2010) 1–4.
[48] S. Ilhan, J. Chem. Res. 12 (2009) 766–769.
[49] S. Ilhan, J. Chem. Res. 6 (2010) 304–306.
[50] S. Ilhan, H. Temel, S. Paşa, I. Tegin, Russ. J. Inorg. Chem. 55 (2010) 1402–1409.
[51] S. Ilhan, Russian J. Coord. Chem. 35 (2009) 347–351.
[52] Gaussian 09, Revision C.01, M.J. Frisch, G.W. Trucks, H. B. Schlegel, G.E. Scuseria, M.A. Robb, J.R. Cheeseman, G. Scalmani, V. Barone, B. Mennucci, G.A. Petersson, H. Nakatsuji, M. Caricato, X. Li, H.P. Hratchian, A.F. Izmaylov, J. Bloino, G. Zheng, J.L. Sonnenberg, M. Hada, M. Ehara, K. Toyota, R. Fukuda, J. Hasegawa, M. Ishida, T. Nakajima, Y. Honda, O. Kitao, H. Nakai, T. Vreven, J.A. Montgomery, Jr.J.E. Peralta, F. Ogliaro, M. Bearpark, J.J. Heyd, E. Brothers, K.N. Kudin, V.N. Staroverov, T. Keith, R. Kobayashi, J. Normand, K. Raghavachari, A. Rendell, J.C. Burant, S.S. Iyengar, J. Tomasi, M. Cossi, N. Rega, J.M. Millam, M. Klene, J.B. Knox, V. Cross, C. Bakken, J. Adamo, R. Jaramillo, R.E. Gomperts, O. Stratmann, J.E. Yazyev, A.J. Austin, R. Cammi, C. Pomelli, J.W. Ochterski, R.L. Martin, K. Morokuma, V.G. Zakrzewski, G.A. Voth, P. Salvador, J.J. Dannenberg, S. Dapprich, A.D. Daniels, O. Farkas, J.B. Foresman, J.V. Ortiz, J. Cioslowski, D.J. Fox, Gaussian Inc, Wallingford, CT, 2010.
[53] P. Hohenberg, W. Kohn, Phys. Rev. 136 (1964) B864–B871.
[54] T.A. Keith, R.F.W. Bader, Chem. Phys. Lett. 194 (1992) 1–8.
[55] C.C. Roothaan, J. Rev, Mod. Phys. 23 (1951) 69–89.
[56] F. London, J. Phys. Radium 8 (1937) 397–409.
[57] R. McWeeny, Phys. Rev. 126 (1962) 1028–1034.
[58] R. Ditchfield, Mol. Phys. 27 (1974) 789–807.
[59] K. Wolinski, J.F. Hilton, P. Pula, J. Am. Chem. Soc. 112 (1990) 8251–8260.
[60] J.R. Cheeseman, G.W. Trucks, T.A. Keith, M.J. Frisch, J. Chem. Phys. 104 (1996) 5497–5509.
[61] P.B. Nagabalasubramaniana, M. Karabacak, S. Periandy, Spectrochim. Acta, Part A 82 (2011) 169–180.
[62] I. Cakmak, J. Mol. Struct. Theochem. 716 (2005) 143–148.
[63] H. Yuksek, I. Cakmak, S. Sadi, M. Alkan, H. Baykara, Int. J. Mol. Sci. 6 (2005) 219–229.
[64] H. Yuksek, M. Alkan, S. Bahceci, I. Cakmak, Z. Ocak, H. Baykara, O. Aktas, E. Agyel, J. Mol. Struct. 873 (2008) 142–148.
[65] S.W. Hwang, Y. Chen, Macromolecules 35 (2002) 5438–5443.
[66] M. Sönmez, M. Çelebi, A. Levent, I. Berber, Z. Şentürk, J. Coord. Chem 63 (2010) 1986–2001.
[67] M. Sönmez, M. Çelebi, A. Levent, I. Berber, Z. Şentürk, J. Coord. Chem 63 (2010) 848–860.
[68] P. Zanello, Inorganic Electrochemistry; Theory, Practice and Application, The Royal Society of Chemistry, Cambridge, 2003.
[69] M.S. Agirtas, I. Gumus, V. Okumus, A. Dundar, ZAAC 638 (2012) 1868–1872.
[70] M.S. Agirtas, B. Cabir, S. Ozdemir, Dyes Pigm. 96 (2013) 152–157.
[71] A. Zalkin, D.H. Templeton, D.G. Karraker, Inorg. Chem. 8 (1969) 26802684.
[72] E. Fleischer, S. Hawkinson, J. Am. Chem. Soc. 89 (1967) 720–721.
[73] G. Kumar, S. Devi, R. Johari, D. Kumar, Eur. J. Med. Chem. 52 (2012) 269–274.
[74] K. Miyoshi, J. Wang, T. Mizuta, Inorg. Chim. Acta 228 (1995) 165–172.
[75] U. Demirbas, R. Bayrak, M. Piskin, H.T. Akcay, M. Durmus, H. Kantekin, J. Organomet. Chem. 724 (2013) 225–261.
[76] O. Kocyigit, A.N. Kursunlu, E. Guler, J. Hazard. Mat. 183 (2010) 29–34.
[77] A.H. Kianfar, S. Ramazani, R.H. Fath, M. Roushani, Spectrochim. Acta Part A. 105 (2013) 374–382.